Robotica (1999) volume 17, pp. 675–683. Printed in the United Kingdom © 1999 Cambridge University Press

A general dynamic model for a large-scale 2-DOF planar parallel manipulator

Khaled R. Atia and M.P. Cartmell

Department of Mechanical Engineering, University of Glasgow, Glasgow, Scotland G12 8QQ (UK)

(Received in Final Form: April 24, 1999)

SUMMARY

In this work a new concept of designing two degree of freedom (2-DOF) planar parallel manipulators (PPMs) is presented. With this design the manipulator's workspace can be increased by increasing the number of *cells* in the manipulator. A general dynamic model is formulated for the manipulator with any number of cells. The model is adapted for *SCARA* and *ADEPT* configurations, and a new approach for balancing these type of manipulators is proposed.

KEYWORDS: Multi-Cell robots: Planar parallel manipulators; Junctions; Cells; Cross-Links.

1. INTRODUCTION

Parallel manipulators display particularly useful characteristics over those of serial devices such as high precision, high load capacity, high rigidity, and high speed capability. Because of this these structures have received a lot of attention as practical alternatives for conventional serial robots. Many researchers, (see for instance[1–3]), have addressed the concept of parallel actuated mechanisms. McColy[4] performed a comparison between a two-link serial driven manipulator and different 2DOF PPMs. The parallel linkages used in the comparison were based on a planar five-bar mechanism. Jean[5] studied static balancing of planar 1, 2 and 3 DOF parallel manipulators. The determination of the singularity loci and the evaluation of the workspace of these planar manipulators were carried out by Gosselin[6] and Merlet,[7] respectively.

In the literature it is shown extensively that the performance of parallel manipulators can be further improved by using redundant actuation. A manipulator with actuation redundancy has more actuators than the number of degrees of freedom required to define its dynamics. However, this makes the selection of the motor torques (in order to follow a desired path) indeterminate. This allows the optimisation of the torque distribution among the actuators according to a certain performance criterion. The search for a solution for actuation redundancy has been addressed by several researchers, Nakamura[8] and Beiner.[9] Kock[10] removed the rotational degree of freedom of the movable platform of a 3-DOF planar manipulator and considered the system as a redundant 2-DOF manipulator. In this case he added a redundant branch and redundant motor to the normal five-bar mechanism. On the other hand in the review by Tadokoro[11] the specific control problem of parallel manipulators was addressed.

Despite the advantages of parallel manipulators there are certain disadvantages to be encountered such as complicated kinematics and dynamics, many singular configurations, and poor workspace availability. Resolution of the latter is very important for any manipulator design. If we restrict ourselves to a 2-DOF parallel robot (a five-bar linkage for example) we will find that the link lengths limit the workspace. On the other hand, there will necessarily be a design limitation of some sort on the link lengths. Also one must have a compact design which is capable of full manoeuvring.

To overcome the limitations of the workspace of the conventional 2-DOF PPMs this work presents a new approach for increasing the workspace without affecting the degrees of freedom of the manipulator. The approach has been inspired by some of the truss-type mechanisms found in the literature.[12]

2. MULTI-CELL PARALLEL 2-DOF MECHANISMS

If attention is initially restricted to revolute type mechanisms the conventional 2-DOF parallel manipulator can be considered as a five-bar linkage with two rotary inputs as shown in Figure 1. If the distance $e = 0$ and all links have the same length, the mechanism becomes the well-known pantograph linkage (Figure 2). If we now consider that linkage as a unit cell and then arrange several such cells in series a multi-cell manipulator is constructed. In this way the number of degrees of freedom is not changed and the resulting workspace is equal to the number of cells multiplied by the original cell's workspace. Figure 3 shows a SCARA type manipulator in which this concept is applied. In fact using the pantograph as the main cell for the manipulator can be profitable; this being due to the simplified constraints and the symmetric characteristics of this configuration. Also it is found[4] that the maximum workspace for the five-bar mechanism is obtained for the case in which the distance $e = 0$.

3. SINGULARITY ANALYSIS OF THE MANIPULATOR

Since all the cells are the same the results of singularity analysis of one cell are the same for the whole manipulator. From Figure 2, and using the results of Damien et al.,[13] the direct-kinematic and the inverse-kinematic matrices of the cell are as follows:

https://doi.org/10.1017/S0263574799001794 Published online by Cambridge University Press

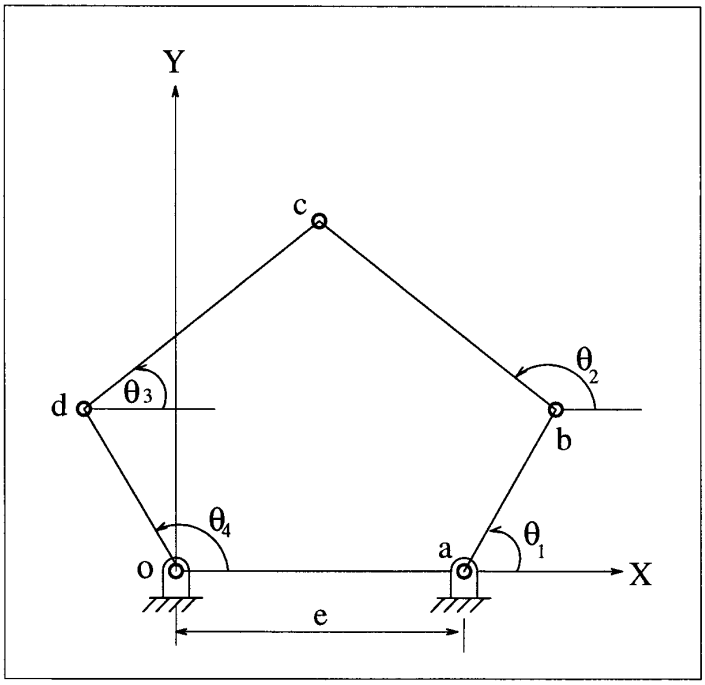


Fig. 1. Five-bar linkage with two rotary inputs.

$$A = \begin{bmatrix} 2L\cos\theta_3 & 2L\cos\theta_4 \\ 2L\sin\theta_3 & 2L\sin\theta_4 \end{bmatrix} \text{ and}$$

$$B = \begin{bmatrix} 4L^2\sin(\theta_4 - \theta_1) & 0 \\ 0 & 4L^2\sin(\theta_3 - \theta_2) \end{bmatrix}$$

A singularity occurs whenever the determinant of A or B, or both, vanishes. When $|\mathrm{B}| = 0$ the manipulator is in a serial singularity and there is a direction along which no Cartesian velocity can be produced. On the other hand when $|\mathrm{A}| = 0$ the manipulator is in a parallel singularity and the manipulator becomes uncontrollable. For our case the determinants of A or B are as follows

$$|\mathrm{A}| = 4L^2\sin(\theta_4 - \theta_3)$$

$$|\mathrm{B}| = 16L^4\sin(\theta_4 - \theta_1)\sin(\theta_3 - \theta_2)$$

From the geometrical structure of the main cell it can be deduced that:

$\theta_4 = \theta_2$ and $\theta_3 = \theta_1$ which leads to

$|\mathrm{A}| = 4L^2\sin(\theta_2 - \theta_1)$ and $|\mathrm{B}| = -16L^4\sin^2(\theta_2 - \theta_1)$

i.e. $|B| = -|A|^2$

This means that both the determinants of A and B vanish for

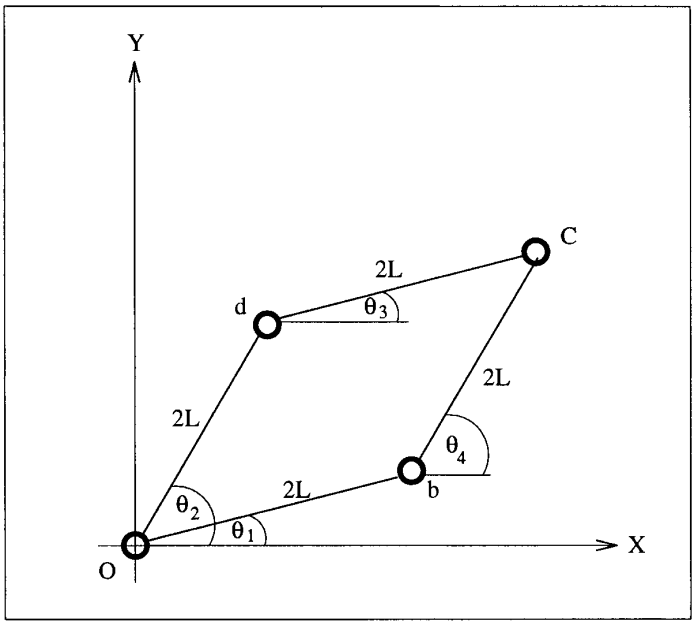


Fig. 2. Main cell (Pantograph Linkage).

https://doi.org/10.1017/S0263574799001794 Published online by Cambridge University Press

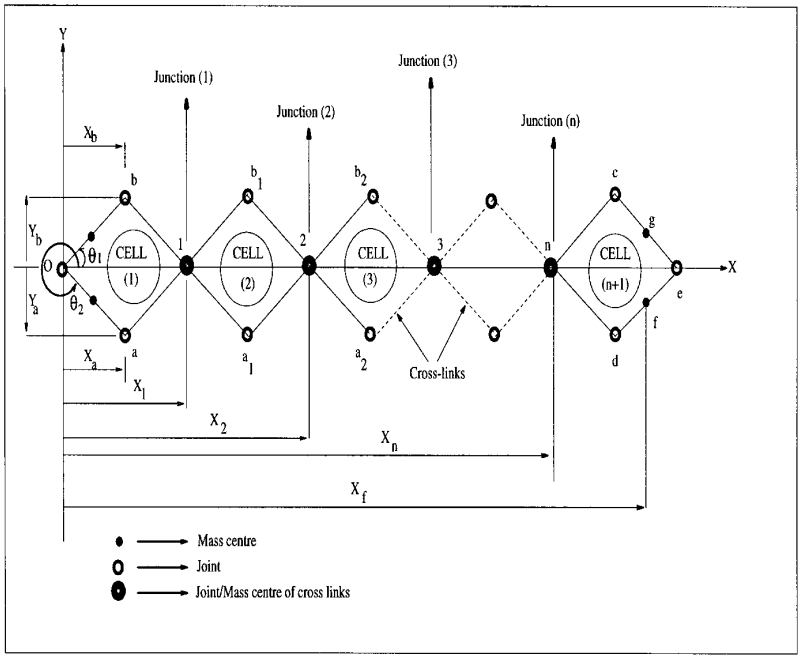


Fig. 3. Multi-Cell 2-DOF parallel manipulator, SCARA configuration.

the same condition, which is $\theta_2 - \theta_1 = k\pi$ where $k = 0,1$ (assuming restrictions on θ_2 and θ_1). At the first value of k the manipulator is fully extended and it demonstrates both parallel and serial singularities. On the other hand when $k = 1$ the manipulator demonstrates both singularities, but in this case the end-effector (point c) overlaps the origin at point O. According to reference 13 the boundaries of the joint and Cartesian spaces are defined by the conditions for parallel and serial singularities respectively. In our case both the boundaries are defined at $k = 0$ and k = 1.

4. DYNAMIC MODELLING OF THE MANIPULATOR

4.1. The SCARA Configuration

The initial assumption is that the manipulaor has n + 1 cells, where n is the number of junctions in the manipulator, and a junction is defined as the point (joint) betwen two adjacent cells. The overall manipulator contains four links (Oa, Ob, de and ce) each having a mass m, a polar moment of inertia about th centre of mass J and a length 2L. There are also 2n cross-links each with a mass 2m, a polar moment of inertia about the centre of mass J_c and a length 4L.

Assuming uniform rigid links yields

$$J = \frac{1}{3} mL^2 \tag{1}$$

$$J_c = \frac{1}{3}\left[2m(2L)^2 \right] = 8J \tag{2}$$

The Lagrange formulation is used to generate the equations of motion:

$$\tau_i = \frac{d}{dt}\left(\frac{\partial T}{\partial \omega_i} \right) - \frac{\partial T}{\partial \theta_i} \text{ for i} = 1,2$$

Where,

T is the total kinetic energy of the robot.
θ_i is the generalised co-ordinate of link i.
ω_i is the angular velocity of link i.
τ_i is the generalised force in the direction of the generalised co-ordinate.

The kinetic energies of the actuated links (Oa and Ob) can be calculated as follows,

$$T_{Oa} = \frac{1}{2}(I_O)_{Oa}\omega_1^2 \text{ and } T_{Ob} = \frac{1}{2}(I_O)_{Ob}\omega_2^2$$

where,

T_{Oa}, T_{Ob} are the kinetic energies of links Oa and Ob, respectively,

ω_1, ω_2 are the angular velocities of link Oa and Ob, respectively.

$(I_O)_{Oa}$, $(I_O)_{Ob}$ are the polar moment of inertia of links Oa and Ob about point O.

The symmetry of links Oa and Ob leads to,

$$(I_O)_{Oa} = (I_O)_{Ob} = J + mL^2 = 4J$$

So,

$$T_{OA} = 2J\omega_1^2 \tag{3}$$

and

$$T_{ob} = 2J\omega_2^2 \tag{4}$$

Now, let

https://doi.org/10.1017/S0263574799001794 Published online by Cambridge University Press

x_j, y_j be the x-y co-ordinates of point j.
j be an identifier assigned to a point.
v_j be the absolute resultant velocity of point j.

From Figure 3, it is clear that:

$$x_1 = 2L(\cos\theta_1 + \cos\theta_2) \text{ and } y_1 = 2L(\sin\theta_1 + \sin\theta_2)$$

Differentiating these with respect to time and then determining the absolute resultant velocity leads to,

$$\nu_1^2 = 4L^2\left\{\omega_1^2 + \omega_2^2 + 2\omega_1\omega_2\cos(\theta_2 - \theta_1)\right\} \quad (5)$$

At every junction, there are two masses representing the two cross-links connected at that junction. These two masses have the same translational velocity. On the other hand, one of the cross-links has an angular velocity ω_1 and the other has an angle velocity ω_2.

From the aforementioned

$$T_1 = 2\left[\frac{1}{2}(2m)\nu_1^2\right] + \frac{1}{2}J_c\omega_1^2 + \frac{1}{2}J_c\omega_2^2 = 2m\nu_1^2 + 4J(\omega_1^2 + \omega_2^2) \quad (6)$$

Where

T_1 is the kinetic energy of the cross-links at junction 1.

Similarly

$$T_2 = 2m\nu_2^2 + 4J(\omega_1^2 + \omega_2^2),\ T_3 = 2m\nu_3^2 + 4J(\omega_1^2 + \omega_2^2),$$
$$T_n = 2m\nu_n^2 + 4J(\omega_1^2 + \omega_2^2)$$

Now let T_{tc} be the total kinetic energy of all cross-links at the n junctions.

So,

$$T_{tc} = T_1 + T_2 + T_3 + T_4 + T_5 + \cdots\cdots + T_{n-1} + T_n$$

Leading to

$$T_{tc} = 4Jn(\omega_1^2 + \omega_2^2) + 2m(\nu_1^2 + \nu_2^2 + \nu_3^2 + \nu_4^2 + \nu_5^2 + \cdots\cdots + \nu_{n-1}^2 + \nu_n^2) \quad (7)$$

From the structure of the manipulator it can be deduced that:

$x_2 = 2x_1,\ x_3 = 3x_1,\ x_4 = 4x_1,\ x_5 = 5x_1$ which leads to: $x_n = nx_1$ (8)

Also,

$$y_2 = 2y_1,\ y_3 = 3y_1,\ y_4 = 4y_1,\ y_5 = 5y_1$$

which leads to:

$$y_n = ny_1 \quad (9)$$

Differentiating these with respect to time and calculating the absolute resultant velocity at each junction gives

$$\nu_2 = 2\nu_1,\ \nu_3 = 3\nu_1,\ \nu_4 = 4\nu_1,\ \nu_5 = 5\nu_1 \text{ and } \nu_n = n\nu_1 \quad (10)$$

from equations (10) and (7)

$$T_{tc} = 4Jn(\omega_1^2 + \omega_2^2) + 2m\nu_1^2\left[\frac{1}{6}n(n+1)(2n+1)\right]$$

Substituting for ν_1 from equation (5) leads to

$$T_{tc} = 4Jn(\omega_1^2 + \omega_2^2)[n + n(n+1)2n + 1)] + 8Jn(n+1)(2n+1)\omega_1\omega_2\cos(\theta_2 - \theta_1) \quad (11)$$

Assuming that there is an imaginary junction at point e, i.e. point e is taken to be the junction number $n+1$ in the system.

So, from equations (8) and (9),

$$x_e = x_{n+1} = (n+1)x_1 \text{ and } y_e = y_{n+1} = (n+1)y_1 \quad (12)$$

Since,

$$x_f = x_e - L\cos\theta_2 = 2(n+1)L\cos\theta_1 + (2n+1)L\cos\theta_2 \quad (13)$$

and

$$y_f = y_e - L\sin\theta_2 = 2(n+1)L\sin\theta_1 + (2n+1)L\sin\theta_2 \quad (14)$$

Differentiating these with respect to time and then calculating the absolute resultant velocity yields

$$\nu_f^2 = 4(n+1)^2L^2\omega_1^2 + (2n+1)^2L^2\omega_2^2 + 4(n+1)(2n+1)L^2\omega_1\omega_2\cos(\theta_2 - \theta_1) \quad (15)$$

Similarly it can easily be deduced that

$$\nu_g^2 = 4(n+1)^2L^2\omega_2^2 + (2n+1)^2L^2\omega_1^2 + 4(n+1)(2n+1)L^2\omega_1\omega_2\cos(\theta_2 - \theta_1) \quad (16)$$

Next, in order to find the contributions of links de and ce we define kinetic energies as follows,

T_{de}, T_{ce} are the kinetic energies of links de and ce, respectively.

$$T_{de} = \frac{1}{2}m\nu_f^2 + \frac{1}{2}J\omega_2^2 \text{ and } T_{ce} = \frac{1}{2}m\nu_g^2 + \frac{1}{2}J\omega_1^2$$

So, from equations (15) and (16) we find,

$$T_{de} = 6J(n+1)^2\omega_1^2 + \frac{1}{2}J[3(2n+1)+1]\omega_2^2 + 6J(n+1)(2n+1)\omega_1\omega_2\cos(\theta_2 - \theta_1) \quad (17)$$

$$T_{ce} = 6J(n+1)^2\omega_2^2 + \frac{1}{2}J[3(2n+1)+1]\omega_1^2 + 6J(n+1)(2n+1)\omega_1\omega_2\cos(\theta_2 - \theta_1) \quad (18)$$

Therefore from the foregoing the total kinetic energy of the system can be determined, thus, $T = T_{Ob} + T_{Oa} + T_{de} + T_{ce} + T_{tc}$ which leads to

$$T = J\xi\omega_1^2 + J\xi\omega_2^2 + J\psi\omega_1\omega_2\cos(\theta_2 - \theta_1) \quad (19)$$

Where

$\xi = (8n^3 + 24n^2 + 26n + 10)$ and $\psi = (16n^3 + 48n^2 + 44n + 12)$

https://doi.org/10.1017/S0263574799001794 Published online by Cambridge University Press

Applying Lagrange's equations yields,

$$\tau_1 = 2\xi J\ddot{\theta}_1 + \psi J\cos(\theta_2 - \theta_1)\ddot{\theta}_2 - \psi J\sin(\theta_2 - \theta_1)\omega_2^2 \quad (20)$$

$$\tau_2 = 2\xi J\ddot{\theta}_2 + \psi J\cos(\theta_2 - \theta_1)\ddot{\theta}_1 + \psi J\sin(\theta_2 - \theta_1)\omega_1^2 \quad (21)$$

Transferring equations (20) and (21) to state space form requires the following substitutions,

$$\dot{\theta}_1 = x_1,\ \theta_1 = x_2,\ \dot{\theta}_2 = x_3 \text{ and } \theta_2 = x_4. \quad (22)$$

So

$$\frac{\tau_1}{J} = 2\xi\dot{x}_1 + \psi\cos(x_4 - x_2)\dot{x}_3 - \psi\sin(x_4 - x_2)x_3\dot{x}_4 \quad (23)$$

and

$$\frac{\tau_2}{J} = 2\xi\dot{x}_3 + \psi\cos(x_4 - x_2)\dot{x}_1 + \psi\sin(x_4 - x_2)x_1\dot{x}_2 \quad (24)$$

By writing equations (22–24) in matrix form we get,

$$\begin{bmatrix} 2\xi & 0 & \psi\cos\Delta x & -\psi x_3\sin\Delta x \\ 0 & 1 & 0 & 0 \\ \psi\cos\Delta x & \psi x_1\sin\Delta x & 2\xi & 0 \\ 0 & 0 & 0 & 1 \end{bmatrix} \cdot \begin{bmatrix} \dot{x}_1 \\ \dot{x}_2 \\ \dot{x}_3 \\ \dot{x}_4 \end{bmatrix} = \begin{bmatrix} \frac{\tau_1}{J} \\ x_1 \\ \frac{\tau_2}{J} \\ x_3 \end{bmatrix} \quad (25)$$

Where $\Delta x = x_4 - x_2$.

4.2 The Adept configuration

In this case the manipulator is moving in the vertical plane. Unlike the SCARA design this configuration will become very dangerous at singular points as the manipulator becomes uncontrollable and tends to fall down under its own weight.

Since the manipulator is moving in the vertical plane its potential energy U must be calculated. It is found that

$$U = -mg_oL\phi(\sin\theta_1 + \sin\theta_2) \quad (26)$$

Where $\phi = n^2 + 5n + 4$

And g_o is the acceleration due to gravity.

The equation of motion in this case is as follows

$$\begin{bmatrix} 2J\xi & 0 & \psi J\cos\Delta x & -\psi Jx_3\sin\Delta x \\ 0 & 1 & 0 & 0 \\ \psi J\cos\Delta x & \psi Jx_1\sin\Delta x & 2J\xi & 0 \\ 0 & 0 & 0 & 1 \end{bmatrix} \cdot \begin{bmatrix} \dot{x}_1 \\ \dot{x}_2 \\ \dot{x}_3 \\ \dot{x}_4 \end{bmatrix} = \begin{bmatrix} \tau_1 - mg_oL\phi\cos x_2 \\ x_1 \\ \tau_2 - mg_oL\phi\cos x_4 \\ x_3 \end{bmatrix} \quad (27)$$

5. STATIC BALANCING OF THE MUTI-CELL 2 DOF PPM

In order to perform balancing counter-masses must be added to the manipulator. In fact the traditional way to balance parallel manipulators is to make extensions to the links and to add counter-masses at the end of these extensions.[5,9] Using this approach means that there are many variables to be adjusted. In the work reported here balancing is performed by adding a counter-cell and one counter-mass M, thus reducing the number of parameters to one. The configuration of the counter-cell and the location of the counter-mass are shown in Figure 4. The expression for the potential energy of the counter-system U_{cs} can be written down as follows,

$$U_{cs} = 2mg_oL(2 + \lambda)(\sin\theta_1 + \sin\theta_2) \quad (28)$$

Where

$$\lambda = \frac{M}{m}$$

The condition for complete balancing is found to be

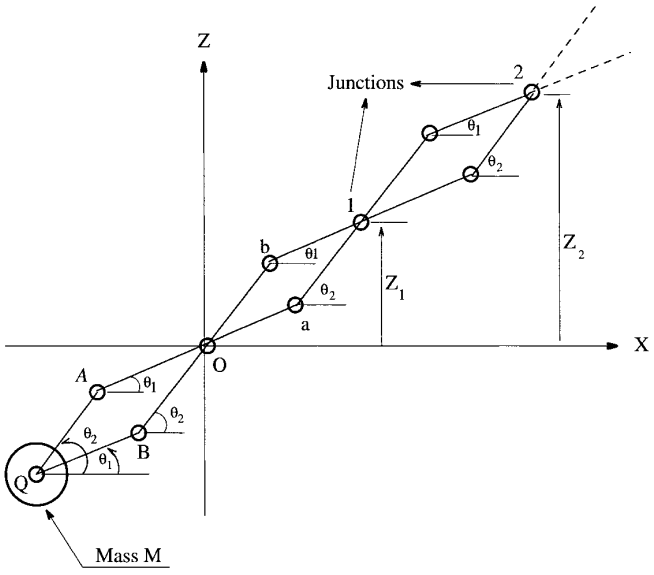


Fig. 4. A part of the balanced manipulator.

https://doi.org/10.1017/S0263574799001794 Published online by Cambridge University Press

$$\lambda = \frac{1}{2} n(n+5) \tag{29}$$

Due to the presence of the counter-system the kinetic energy of the manipulator must be updated and the new equations of motion must be formulated. The updated equations are as follows:

$$\begin{bmatrix} 2\tilde{\xi} & 0 & \tilde{\psi}\cos\Delta x & -\tilde{\psi}x_3\sin\Delta x \\ 0 & 1 & 0 & 0 \\ \tilde{\psi}\cos\Delta x & \tilde{\psi}x_1\sin\Delta x & 2\tilde{\xi} & 0 \\ 0 & 0 & 0 & 1 \end{bmatrix}$$

$$\cdot \begin{bmatrix} \dot{x}_1 \\ \dot{x}_2 \\ \dot{x}_3 \\ \dot{x}_4 \end{bmatrix} = \begin{bmatrix} \frac{\tau_1}{J} \\ x_1 \\ \frac{\tau_2}{J} \\ x_3 \end{bmatrix} \tag{30}$$

Where

$$\tilde{\xi} = 8n^3 + 27n^2 + 41n + 20$$

And

$$\tilde{\psi} = 16n^3 + 54n^2 + 74n + 14$$

6. REAL-TIME SIMULATION OF THE CONTROLLED MANIPULATOR

Due to the fact that parallel manipulators have the merit that they can move at high speeds their dynamics should be used appropriately in any adopted control strategy. In serial robots the computed torque method has often been applied. It is based on the computation of the inverse dynamics for linearization and PID or PD laws to control disturbances and modelling errors. The same method can be applied to the control of parallel manipulators. The key point for its application is how fast the inverse dynamics problem can be solved.

To examine the feasibility of the controller with regard to the proposed manipulator a computed torque controller was applied to a two-cell SCARA type manipulator and the system was simulated using a SIMULINK/dSPACE real time-hardware system. The initial states of the manipulator were as follows:

$$x(0) = \{x_1 = 0,\ x_2 = 0,\ x_3 = 0,\ x_4 = 0.524\ rad\}$$

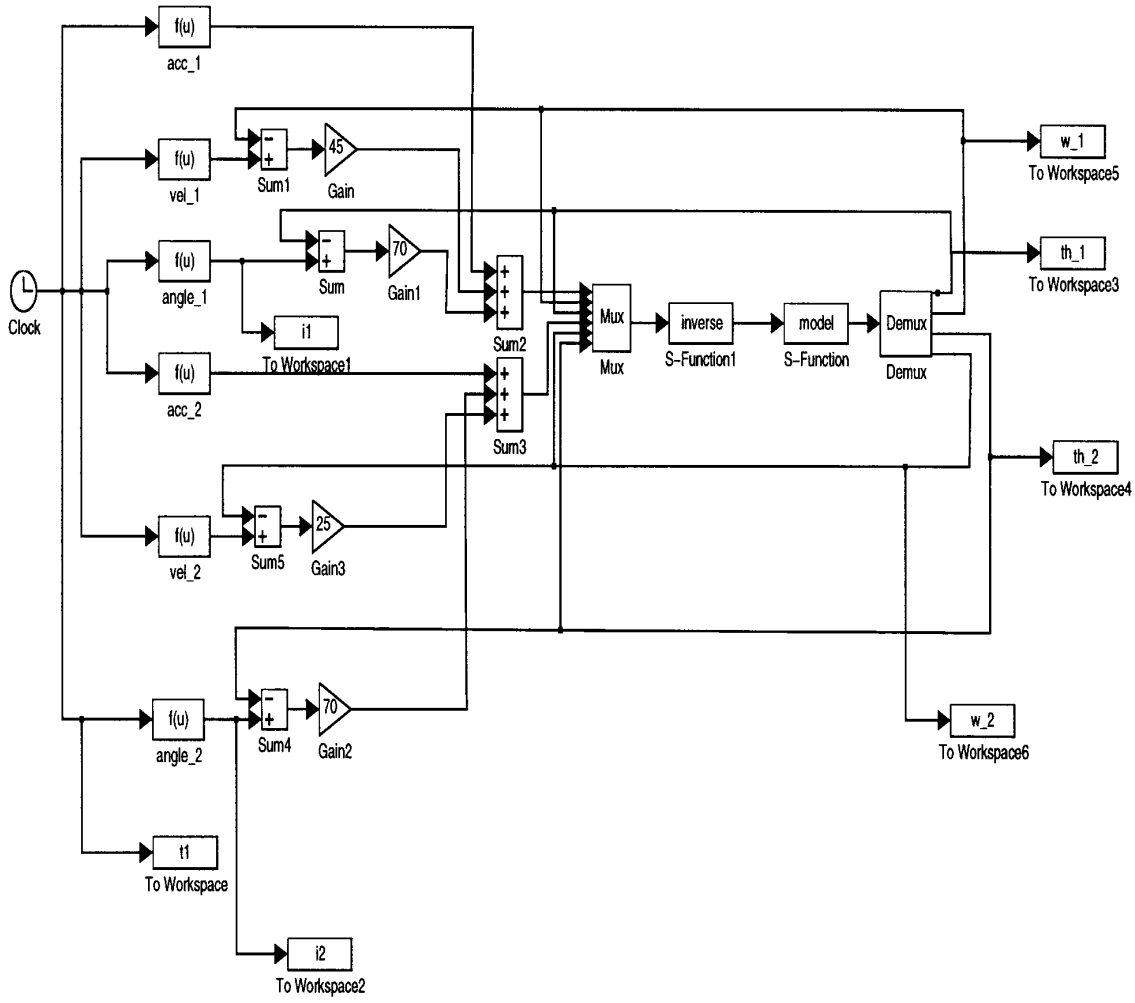


Fig. 5. SIMULINK block diagram of the controlled manipulator.

https://doi.org/10.1017/S0263574799001794 Published online by Cambridge University Press

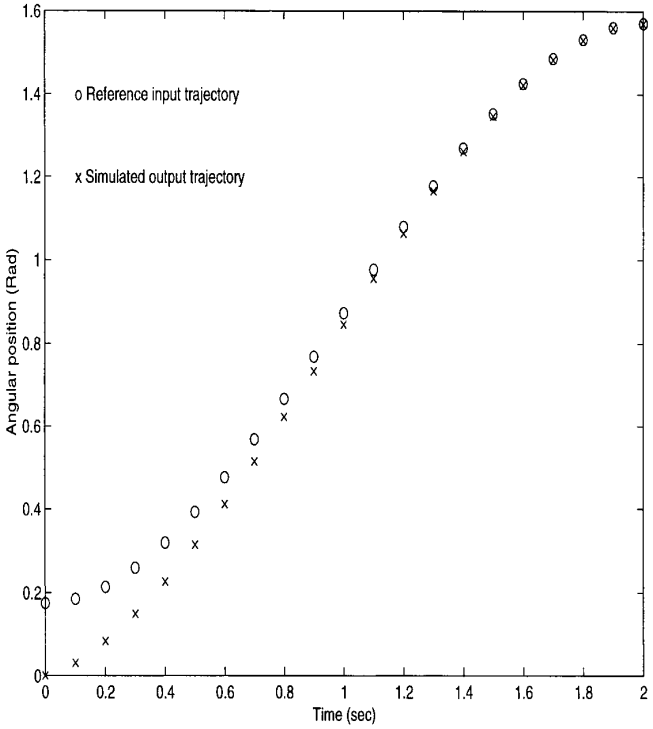


Fig. 6. Response of the first actuated link.

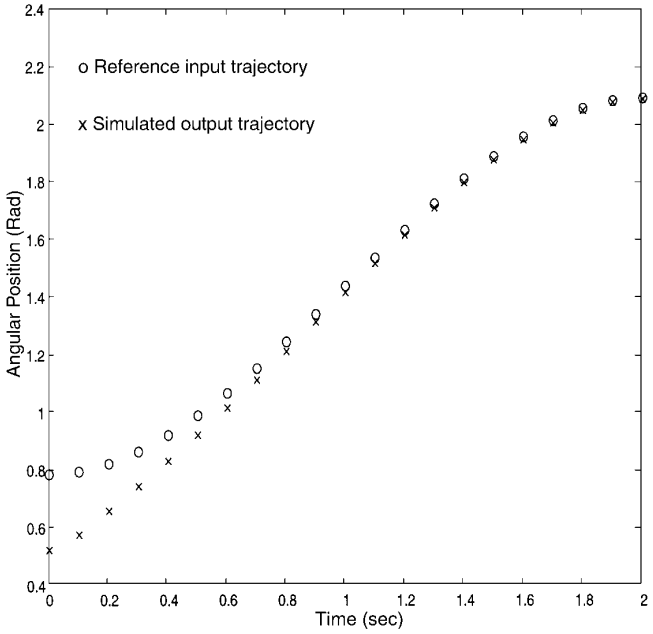


Fig. 7. Response of the second actuated link.

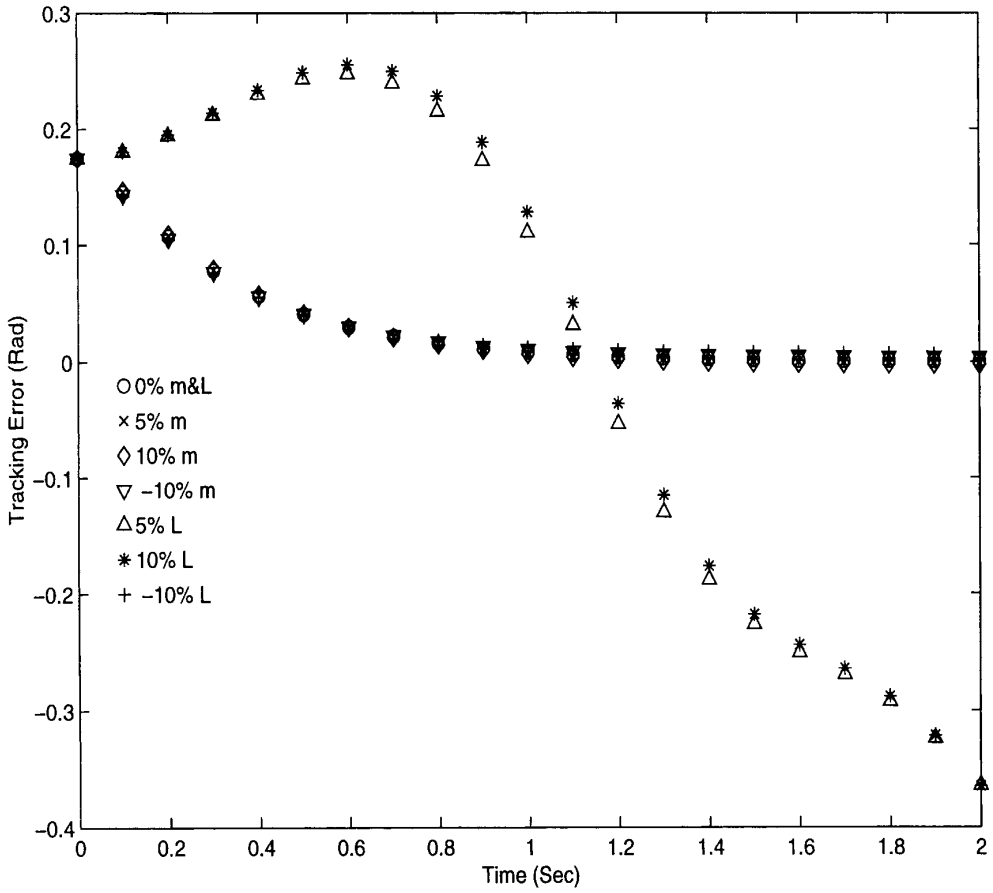


Fig. 8. The effect of parameter change on the tracking error (first actuated link).

https://doi.org/10.1017/S0263574799001794 Published online by Cambridge University Press

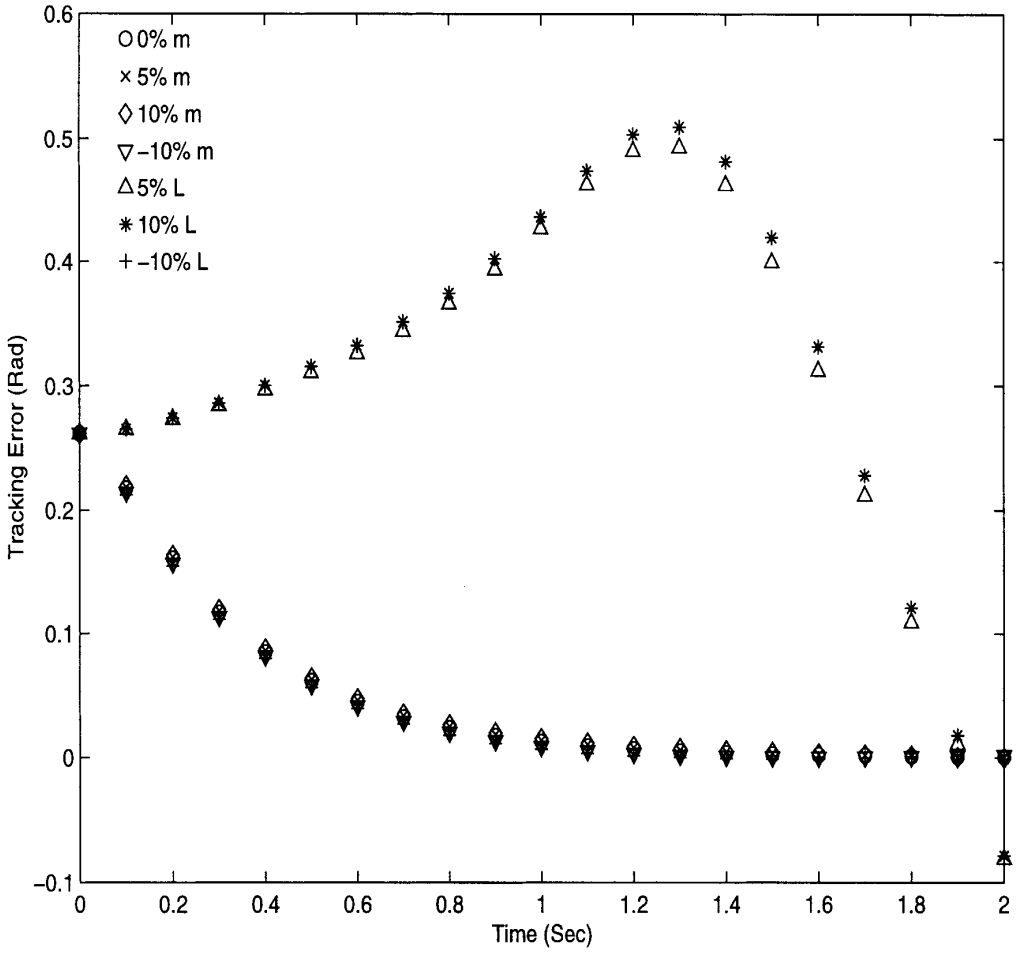


Fig. 9. The effect of parameter change on the tracking error (second actuated link).

A prescribed third order manoeuvre was chosen for the actuated joints. The starting and final destinations of the paths of the two actuated joints were

$$\theta_1(0)=0.01745rad,\ \theta_1(f)=\frac{\pi}{2}\,rad,\ \theta_2(0)$$

$$=\frac{\pi}{4}\,rad \text{ and } \theta_2(f)=\frac{2\pi}{3}\,rad$$

The chosen physical parameter of the manipulator to be used are derived from an experimental system designed and built by the authors at Glasgow university, and are as follows,

$$m=0.241Kg \quad L=0.125\text{m} \quad \text{and} \quad J=0.00126\ Kg.\text{m}^2$$

The block diagram of the controller is shown in Figure 5. The controller gains are adjusted to give a critical damped response and their values are as follows,

$$K_{p1}=70,\ \ K_{D1}=45,\ \ K_{p2}=70 \text{ and } \mathrm{K_{D2}}=25$$

The simulation results are shown in Figures 6 and 7. The computation time of the system is found to be equal to 0.0001848 second. In fact, this time comprises the computation time of the direct dynamics of the system and the input trajectories. So, the time required for the inverse problem alone is less than the time quoted above, which means that it should be quite efficient for implementation of the controller to the real system.

To check the sensitivity of the controller to parameter change the mass m and the length L are perturbed by amounts equal to 5, 10 and -10%. The simulation results of the tracking errors of the two actuated links in each case, and the case for no perturbations, are shown in Figures 8 and 9. It can be seen that the controller is sensitive only to the increase in the length L.

CONCLUSION

In this paper a new concept for multi-cell planar parallel manipulators has been presented. By means of this design the workspace of the manipulator can be increased by increasing the number of cells. A general dynamic model for this linkage with different manipulator designs was formulated using Lagrange's method. The model depends on a key factor which is the number of junctions in the manipulator. Static balancing of the manipulator was also studied and the condition for complete balancing was derived. It was also found that the computed torque

https://doi.org/10.1017/S0263574799001794 Published online by Cambridge University Press

controller could be efficiently applied to the manipulator given that the time required for computing the inverse dynamic problem is quite small. It is found also that the controller is sensitive only to the increase in the length *L*.

References

1. H. Funabshi, "In parallel actuated mechanisms as a new robotic mechanism". *J. Advanced Robotics* **8**, No. 6, 535–544 (1994).
2. J.P. Merlet, "Parallel manipulators: state of the art and perspectives", *J. Advanced Robotics* **8**, No. 6, 589–596 (1994).
3. Masaru Uchiyama, "Structures and characteristics of parallel manipulators", *J. Advanced Robotics* **8**, No. 6, 545–557 (1994).
4. D. McCloy, "Some comparisons of serial-driven and parallel-driven manipulators", *Robotica* **8**, No. 4, 355–362 (1990).
5. M. Jean and C.M. Gosselin, "Static balancing of planar parallel manipulators", *Proc. of the IEEE Int. conference on Robotics and Automation* (1996) **Vol. 4**, pp. 3732–3737.
6. C.M. Gosselin and J. Wang, "Singularity loci of planar parallel manipulators with revolute actuators", *J. Robotics and Autonomous Systems* **21**, No. 4, 377–398 (1997).
7. Jean-Pierre Merlet, C.M. Gosselin and N. Mouly, "Workspaces of planar parallel manipulators", *J Mechanism and Machine Theory* **33**, No. 1–2, 7–20 (1998).
8. Y. Nakamura and M. Ghodoussi, "Dynamics computation of closed-link robot mechanisms with non-redundant and redundant actuators", *IEEE Trans. on Robotics and Automation* (1989) **Vol. 5**, No. 3, pp. 294–302.
9. L. Biener, "Redundant actuation of a closed-chain manipulator", *J. Advanced Robotics* **11**, No. 3, 233–245 (1997).
10. S. Kock and W. Schumacher, "A Parallel x-y manipulator with actuation redundancy for high-speed and active-stiffness applications", *Proc. of the IEEE Int. Conference on Robotics and Automation* (1998) **Vol. 3**, pp. 2295–2300.
11. S. Tadokoro, "Control of parallel mechanisms", *J. Advanced Robotics* **8**, No. 6, 559–571 (1994).
12. M. Tanaka, "Large-scale framed structure as parallel mechanism with hyper-redundancy", *J. Advanced Robotics* **8**, No. 6, 573–587 (1994).
13. D. Chablat and P. Wenger, "Working modes and aspects in fully parallel manipulators", *Proc. of the 1998 IEEE Int. Conf. On Robotics and Automation* (1998) **Vo. 3**, pp. 1964–1969.

https://doi.org/10.1017/S0263574799001794 Published online by Cambridge University Press